

RESEARCH ARTICLES

Tuning of a wireless power transfer system with a hybrid capacitor array

NURCAN KESKIN AND HUAPING LIU

Power transfer efficiency in loosely coupled inductive systems can be enhanced by resonance. Primary and secondary can be tuned to same resonant frequency. In this paper, MOSFET-based Varactors and switchable capacitors are used for re-tuning of such a system at 13.56 MHz. This is achieved either using each cap structure alone or as a hybrid model. These techniques are designed for 13.56 MHz wireless power transfer system.

Keywords: Wireless power, Inductively coupled, MOSCAP, Tuning, Antenna

Received 19 May 2015; Revised 14 November 2015; Accepted 16 November 2015

I. INTRODUCTION

Wireless power transfer (WPT) is a way of transferring power from one device to another device without any wire or cable connections [1–5]. The technology has become increasingly important with the development of various customer electronics that require frequent charging with very different charging requirements and equipment. Loosely coupled systems [1, 6–8] provide freedom of movement, but they suffer from lower-power transfer efficiencies compared to their strongly coupled counterparts. Applying resonance to the system will increase the power transferred if a robust tuning of both primary and secondary can be achieved and kept. Based on the application and the system, different resonance frequencies are used such as 100 kHz, 6.78 MHz [1–3], and 13.56 MHz [4, 5]. In this paper, two different cap structures are applied to a WPT system to re-tune the circuitry at 13.56 MHz. Section II gives background about inductively coupled systems (ICS). Section III analyzes MOS cap structures. Details of the proposed cap structures are given. Methodology and simulations results are summarized in Section IV. Conclusion is given in Section V.

II. INDUCTIVELY COUPLED SYSTEMS

In ICS [6–8]; the creation of a magnetic field in the near-field of the antenna is the key. The changing magnetic field creates an alternating current (AC) in the primary side. The AC induces a voltage onto the secondary side which in return creates an AC current. Induced voltage is described by

Ampere’s and Faraday’s Laws. Rectification of the AC current on the secondary side results in direct current (DC). Later the DC current is used to charge a load (usually a battery). ICS use mutual inductance (M) model where induced and reflected voltages define the coupling between the primary and secondary. A simple circuit equivalent of an ICS is shown in Fig. 1.

$$V_1 = j(2\pi f)L_1^*I_1 + j(2\pi f)M^*I_2, \quad (1a)$$

$$V_2 = j(2\pi f)L_2^*I_2 + j(2\pi f)M^*I_1. \quad (1b)$$

Induced voltages both at primary and secondary sides can be expressed in terms of M as seen in equations (1a) and (1b), where M is the mutual inductance, k is the coupling coefficient, f is the operation frequency, V_1 is the primary voltage, V_2 is the induced voltage in secondary, I_1 is the primary current, I_2 is the secondary current, L_1 is the self-inductance of primary, and L_2 is the self-inductance of secondary.

A) Leakage inductance

Leakage inductance is an inductive component that is present in an ICS. Any magnetic flux that does not link the primary side to the secondary side will not have any role in system’s power transfer action. This kind of flux will act as inductive impedance in the circuit and called “Leakage inductance”. Loosely coupled systems suffer from leakage inductance (might be larger than the mutual inductance) because of low-coupling coefficient ($k < 0.1$) and substantial air gap [1, 6–8]. By all means, coupling coefficient in equation (2) will vary based on the distance or the alignment of the coils [6–8].

$$k = \frac{M}{\sqrt{L_1 L_2}}. \quad (2)$$

School of Electrical Engineering and Computer Science, Oregon State University, Corvallis, OR 97331-5501, USA

Corresponding author:

N. Keskin

Email: nurcankeskin@gmail.com

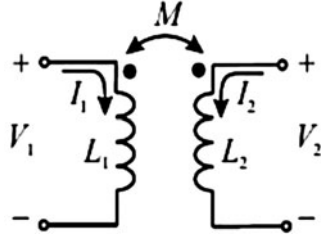


Fig. 1. Mutually coupled inductors.

B) Compensation topologies

Different compensation topologies [9, 10] have been implemented in power systems for years to reduce the effects of leakage inductance therefore increasing the power transfer efficiency and capacity. Including the uncompensated scenario; there are nine common topologies where compensation capacitor is connected either in series or parallel at the primary and/or at the secondary.

These topologies can be listed as UU (uncompensated primary, uncompensated secondary), US, UP, SU, PU, SS (series primary, series secondary), SP, PS, PP (parallel primary, parallel secondary in Fig. 2). It is also possible for primary to have compensation capacitors both in series and parallel at the same time. Based on the requirements and the application; any combination of these can be used. The proposed method in this paper can be used for all of the above topologies except UU.

C) Resonance

In order to enhance the power transfer capability, many WPT systems use the resonance effect [11, 12] where primary and secondary sides resonate at the same frequency. The selection of this frequency changes based on the application, size, cost, and power requirements. Circuit mismatches, load, and magnetic coupling variations can cause deviation from the original $f_{resonance}$ which will require tuning of the circuitry to gain back the optimal working condition again.

III. MOSFET CAPACITORS

Various types of capacitors are used in IC design such as metal-insulated-metal (MIM) capacitors, diode-based capacitors, or MOSFET capacitors (MOSCAP). Among these capacitors, MOSCAP [11] can be used to minimize layout area. The bottom plate of the MOSCAP can be obtained by shorting drain and source terminals of MOSFET device while the gate will be the top plate of the capacitor. By changing the DC bias voltage at the bottom plate, the capacitance value can be varied [13]. Illustration of a MOSCAP along with its

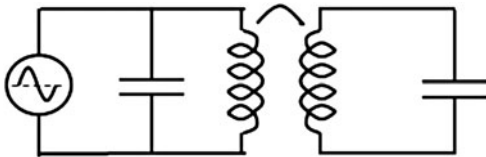


Fig. 2. Parallel primary-parallel secondary WPT System.

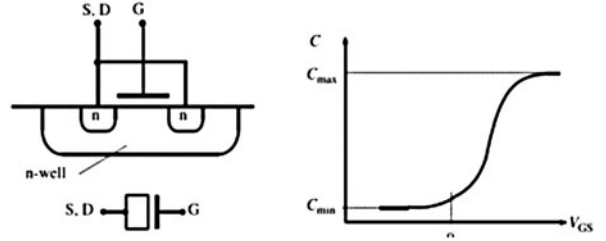


Fig. 3. Sample MOSFET cap and its capacitance change.

capacitance is shown in Fig. 3. Minimum and maximum values are given in equation (3).

$$C_{\min} = \frac{\epsilon_{si}}{t_{dep}} \quad \text{and} \quad C_{\max} = \frac{\epsilon_{ox}}{t_{ox}}, \quad (3)$$

where ϵ_{si} and ϵ_{ox} are the permittivity of the silicon and oxide, respectively. At the same time, t_{dep} and t_{ox} are the thickness of the depletion region in the silicon substrate and oxide between silicon and its gate. Depending on the voltage at the gate terminal (G) versus the source/drain (S, D) combined terminals, the MOSFET device travels in three different operating regions of accumulation, depletion, and inversion [13]. These regions basically carry either the same type of charge under channel as that of the bulk (in accumulation) or different types of charge (in inversion). The depletion region is the transitional operation between the accumulation and the depletion. Therefore, this device can be modeled as a capacitor since during the different operational regions charges at the channel varies based on the voltage potential difference between two terminals (G versus S/D). The variation of the capacitor is shown in Fig. 3. Typical value of the capacitor can be calculated using equation (4).

$$C_{typ} = \frac{Q_{channel}}{V_G - V_{S,D} - V_{th}}, \quad (4)$$

where V_G and $V_{S,D}$ are the voltages at the gate and source/drain terminals, respectively. V_{th} is the threshold of the MOSFET device defined by the semiconductor process. $Q_{channel}$ is the charges stored under the gate at the channel.

IV. METHODOLOGY AND SIMULATION RESULTS

The optimum WPT with different capacitors, inductors, or resistors to re-tune impedance, resonance, or frequency matching circuitry has been constantly investigated [14–19]. The role of a capacitor array and a Varactor in addition to a main capacitor is presented in this paper. The system properties are explained in the next section followed by simulation results and conclusion.

A) System properties

A parallel-primary and parallel-secondary WPT system in Fig. 2 is studied. A sinewave is applied to the primary with 13.56 MHz of frequency and 2 V of peak-to-peak of amplitude. Both primary and secondary self-inductances are chosen as 500 nH, where both sides resonate at 13.56 MHz.

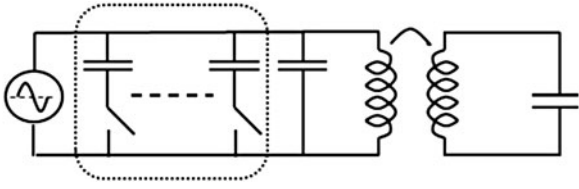


Fig. 4. WPT system with switchable capacitor array (dotted-box).

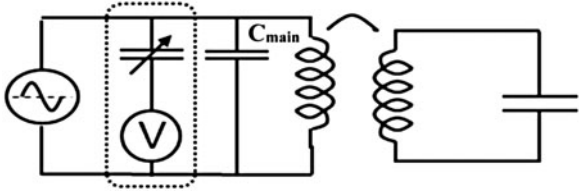


Fig. 5. Varactor (dotted-box)-based WPT system.

It is assumed that system deviates from the designed $f_{resonance}$ (detuned) due to possible various conditions such as distance, leakage inductance, load variations, component tolerance variations, and environmental changes. The main focus of the paper is to study the different capacitor structures for the compensation of the primary and their role on the re-tuning of the system.

B) Proposed capacitor topologies

To provide dynamic tuning of the WPT system, different compensation techniques are used. Switchable capacitor arrays are proposed in [16, 17, 19] as shown in Fig. 4.

A diode-connected variable capacitor structure is used in [16, 18]. Here, Varactor structure based on a MOSCAP of Fig. 3 is utilized as shown in Fig. 5.

In this circuit, C_{main} is the main capacitor and it is directly connected to the primary self-inductor which plays a role in achieving high-Q value. Binary cap arrays or Varactors [20, 21] will have lower-Q value compared with C_{main} due to additional circuit components attached to them such as switches or DC bias voltages, etc.

Tuning range of the Varactor in Cadence simulation results is shown in Fig. 6. The voltage bias (V) of the Varactor in the dotted box of Fig. 5 is varied from -1 to 1 V; hence, $f_{resonance}$ can be tuned accordingly from 11 to 14.9 MHz, where the

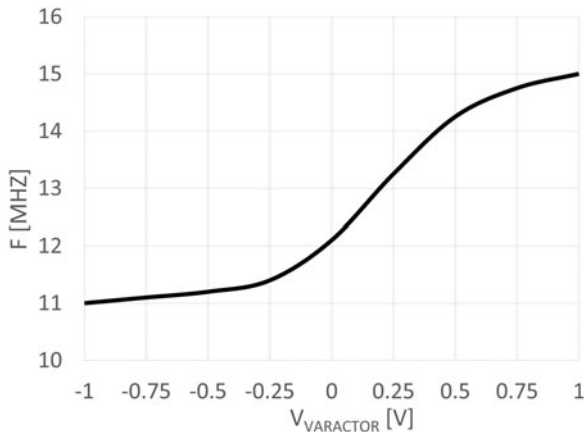


Fig. 6. $f_{resonance}$ versus Varactor bias (V).

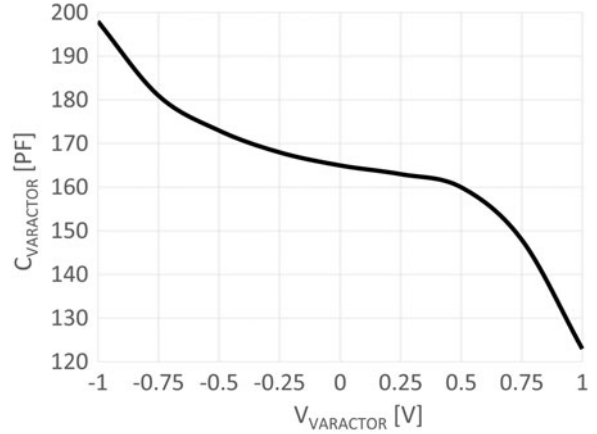


Fig. 7. Capacitance of the MOSCAP (Varactor) versus V_{bias} .

target center frequency is 13.56 MHz. Figure 7 shows the range of MOSCAP from 120 to 200 pF when V is varied to tune the resonance frequency. This corresponds to tunability from -10% to $+10\%$ of nominal value the MOSCAP.

At the same time, as seen in Fig. 6, the saturation happens when V is less than -0.5 V, or more than 0.7 V. Therefore, there is a need to increase tuning range using different architectures such as the hybrid capacitor structure shown in Fig. 8.

The final proposed structure is shown in Fig. 8 where both Varactor and switchable cap arrays are used together for a hybrid model. In this model; while coarse tuning can be achieved by the Varactor section where V is changed to compensate for larger non-idealities of the resonance circuit, switchable capacitor array section can be used to provide fine tuning, so that smaller capacitors are used in the switchable capacitor array to minimize number of capacitors used.

Final total capacitor is equal to

$$C_{total} = C_{main} + C_{switch} + C_{varactor}. \quad (5)$$

The hybrid architecture of Fig. 8 is simulated to show the extended range of tunability using both the switchable binary cap array as well as the Varactor. In this simulation, V of the Varactor is varied from -0.5 to 1 V and the switchable binary cap array is varied from 84 to 240 pF in four steps providing four separate curves in Fig. 9. The maximum frequency is increased up to 19.4 MHz (from 14.9 MHz of Fig. 6 when $V = 1$ V) and lower frequency is further pushed down to 10 MHz (from 11 MHz of Fig. 6 $V = -1$ V). This will provide $-/+35\%$ of tunability range of the resonance frequency around 13.56 MHz.

By using different options of binary cap array together with Varactor, all the values between upper and lower curves can be obtained. In Fig. 9, four different settings of binary cap array are used. As seen in Figs 6 and 9, tuning range by Varactor is a

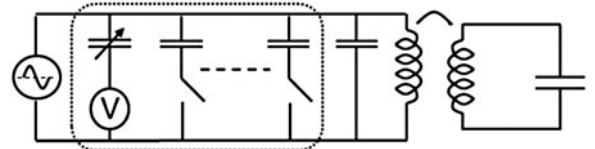


Fig. 8. Hybrid resonance circuit (dotted-box) in WPT system.

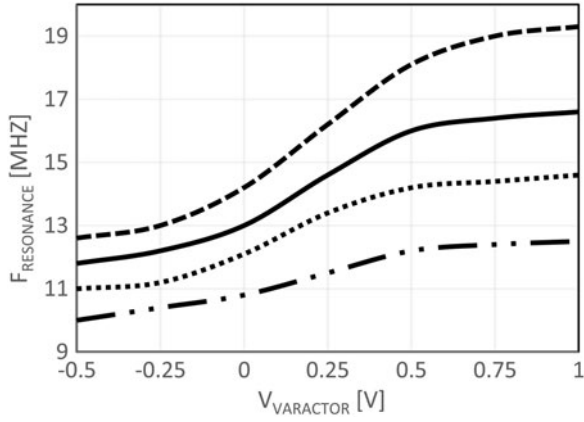


Fig. 9. Extended range of $f_{resonance}$ by varying both the binary cap array and the MOSCAP.

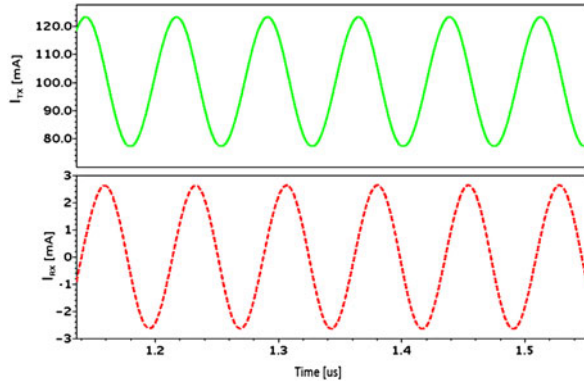


Fig. 10. Transmitter and receiver current.

non-linear (not a straight-line) due to the nature of the MOSCAP. Using binary cap array provides finer steps, linear transitioning points, and extended range. Figure 10 shows the current signal transmitted from the transmitter antenna ($I_{TX} = 45 \text{ mA}_{pp}$) and current signal received at the receiver antenna ($I_{RX} = 5 \text{ mA}_{pp}$). Figure 11 shows voltage waveform at the transmitter antenna ($V_{TX} = 2 \text{ V}_{pp}$) and voltage waveform at the receiver antenna ($V_{RX} = 0.2 \text{ V}_{pp}$). At the same time, the resonant current through the Varactor is 20 mApp and the resonant current on the

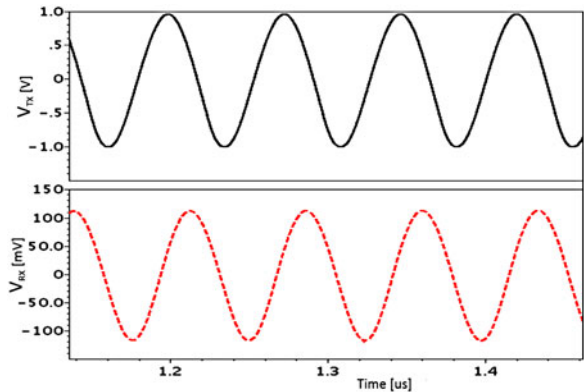


Fig. 11. Transmitter and receiver voltage.

Table 1. Circuit element values of different primary structures.

Circuit	C_{main} (pF)	C_{switch} (pF)	$C_{varactor}$ (pF)	L_{tx} (nH)	L (nH)	V (V)
Baseline	138	–	164	500	0	0
Non-ideal	138	–	164	500	100	0
Hybrid	92	46	164	500	100	0.1

binary cap is 25 mApp. The power rating of the Varactor in this setup is 40 mW.

C) Detuning and simulation results

The values of circuit elements of the primary are shown in Table 1 for different schemes. As a baseline, an ideal case is considered where there are no losses in the circuit. To detune the circuit, an additional 100 nH is introduced for simulation purposes. This value represents about 20% deviation from the nominal antenna and chosen as an example. In reality, there will be so many detuning values possible due to varying distance and environmental effects between the transmitter and the receiver [3, 4].

Different cap values are used to bring the circuit back to the resonant frequency. Figure 12 shows a simulation result where initially the primary (transmitter side of the system) is tuned to 13.56 MHz. After adding non-idealities in to the circuit, the transmitter power is deviated from the desired resonant peak to the left for the non-ideal case. The proposed hybrid structure is used to bring the resonant frequency back to 13.56 MHz, so that resonant peak of the transmitter aligns with that of the receiver.

The received power signals of baseline, non-ideal and hybrid schemes in frequency domain when coupling coefficient (k) is equal to 0.1 is shown in Fig. 13. Received power is improved and it is only 0.12 dB away from the baseline when the power level is about -18 dB level.

A different leakage inductance value (200 nH) is used for following simulations. In order to find the optimum value, both V (0.1–0.2 V) of the Varactor and also number (1–6) of binary capacitors are swept as seen in Fig. 14. It was observed that the largest received power is when V is equal to 200 mV and number of binary capacitors is 4, which is about 30 pF of binary cap value for this particular leakage

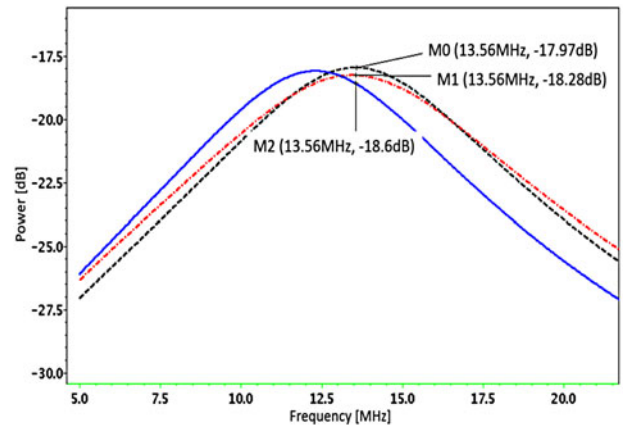


Fig. 12. Transmitted power of baseline (dashed), non-ideal (solid), and hybrid (dashed/dotted).

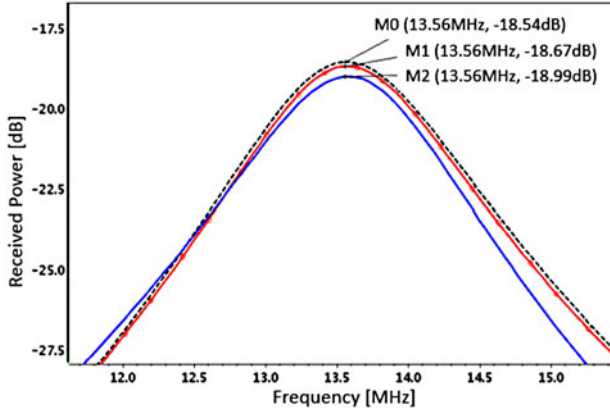


Fig. 13. Received power of baseline (dashed), non-ideal (solid), and Hybrid (solid with dots) when $k = 0.1$.

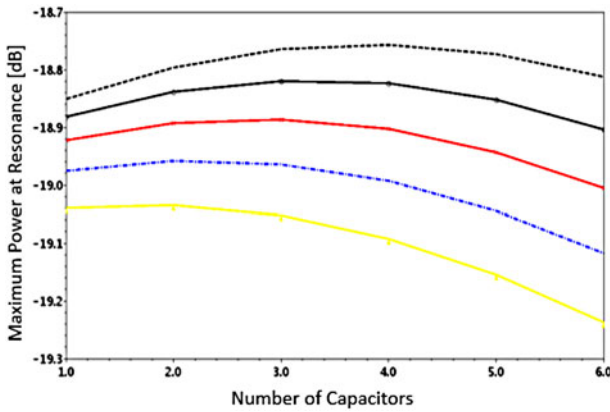


Fig. 14. Received power of Hybrid architecture when $k = 0.1$, $L_{leakage} = 200$ nH versus V and number of binary cap.

inductance. With bigger leakage inductance, the received power by the proposed hybrid architecture is improved to more than 1 dB level as seen in Fig. 15.

In Table 2, resonance tuning range and size of capacitors are compared [22–25]. It is noted that [23] tunes the system in both transmitter side as well as in the receiver side using the same size of capacitor array.

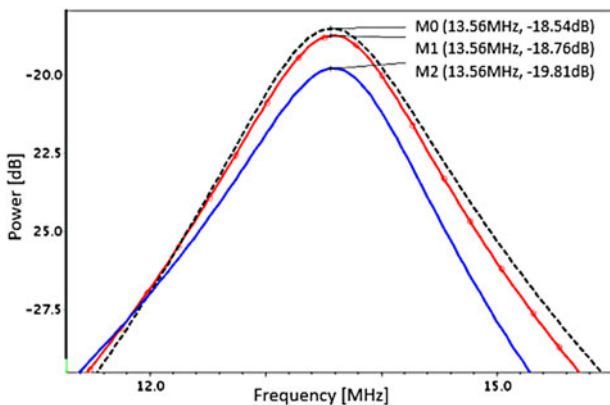


Fig. 15. Received power of Hybrid ($k = 0.1$, $L_{leakage} = 200$ nH).

Table 2. Comparison of capacitive tuning WPT systems.

References	Fcenter (MHz)	Tuning range	C_{main}	C_{switch} range	C_{moscap}
[22]	13.84	Not available	158 pF	95–374 pF	None
[23]	13.56	$\mp 46\%$	213 pF	9–470 pF	None
[24]	2400	$\mp 10\%$	6 pF	None	26–70.7 fF
[25]	0.085	$\mp 7\%$	175 nF	1.6–52 nF	None
This work	13.56	$\mp 35\%$	92 pF	21–84 pF	120–164 pF

V. CONCLUSION

Detuning of a WPT system is an important issue that affects overall power transfer efficiency. Dynamic tuning of these systems under various conditions is studied extensively in literature. In this paper, it is shown that Varactor and switch array capacitors can be used individually or together as a hybrid model to de-tune a WPT system. Varactor type has an advantage of saving layout area while switch array caps can provide fine tuning. Hybrid model can be used for the WPT applications in the MHz range to provide an optimum trade-off, where the quality is optimized using C_{main} as a fixed capacitor. This architecture is successfully designed at 13.56 MHz. The tunability range of the resonance frequency is greatly extended around 13.56 MHz.

REFERENCES

- [1] Tseng, R.; Novak, B.V.; Shevde, S.; Grajski, K.A.: Introduction to the alliance for wireless power loosely-coupled wireless power transfer system specification version 1.0, in IEEE Wireless Power Transfer Conf., Technologies, Systems and Applications, Perugia, Italy, 15–16 May (2013), 79–83.
- [2] Riehl, P.S. et al.: Wireless power systems for mobile devices supporting inductive and resonant operating modes. IEEE Trans. Microw. Theory Tech., **63** (3) (2015), 780–790.
- [3] Dai, J.; Ludois, D.C.: A survey of wireless power transfer and a critical comparison of inductive and capacitive coupling for small gap applications. IEEE Trans. Power Electron., (2015), **30**, 1–14.
- [4] Lu, Y.; Li, X.; Ki, W.-H.; Tsui, C.-Y.; Yue, P.: A 13.56 MHz fully integrated 1x/2x active rectifier with compensated bias current for inductively powered devices, in IEEE ISSCC, (2013), 66–68.
- [5] Li, X.; Tsui, C.-Y.; Ki, W.-H.: A 13.56MHz wireless power transfer system with reconfigurable resonant regulating rectifier and wireless power control for implementable medical devices. IEEE J. Solid-State Circuits, **50** (4) (2015), 978–989.
- [6] Stielau, O.H.; Covic, G.A.: Design of loosely coupled inductive power transfer systems, in Proc. Power System Technology, (2000), 85–90.
- [7] Wang, C.-S.; Stielau, O.H.; Covic, G.A.: Load Models and their application in the design of loosely coupled inductive power transfer systems, in Proc. Power System Technology, (2000), 1053–1058.
- [8] Fotopoulou, K.; Flynn, B.W.: Wireless power transfer in loosely coupled links: coil misalignment model. IEEE Trans. Magn., **47** (2) (2011), 416–430.
- [9] Zhou, W.; Hao, M.: Design considerations of compensation topologies in ICPT system, in Applied Electronics Conf., (2007), 985–990.

- [10] Jegadeesan, R.; Guo, Y.-X.: Topology selection and efficiency improvement of inductive power links. *IEEE Trans. Antenna Propag.*, **60** (10) (2012), 4846–4854.
- [11] Mastri, F.; Costanzo, A.; Dionigi, M.; Mongiardo, M.: Harmonic balance design of wireless resonant-type power transfer links, in *IEEE MTT-S Int. Microwave Workshop on Innovative Wireless Power Transmission (IMWS)*, (2012), 245–248.
- [12] Rashidzadeh, R.; Basith, I.I.: A test probe for TSV using resonant inductive coupling, in *IEEE Int. Test Conf.*, (2013), 1–6.
- [13] Hu, C.C.: *Modern Semiconductor Devices for Integrated Circuits*, 1st ed., Prentice-Hall, 2009.
- [14] Ogawa, K.; Oodachi, N.; Obayashi, S.; Shoki, H.: A study of efficiency improvement of wireless power transfer by impedance matching, in *IEEE MTT-S Int. Microwave Workshop on Innovative Wireless Power Transmission (IMWS)*, (2012), 155–157.
- [15] Mercier, P.P.; Chandrakasan, A.: Rapid wireless capacitor charging using a multi-tapped inductively-coupled secondary coil, in *IEEE Trans. Circuits and Systems I Regular Papers*, September (2013), 2263–2272.
- [16] Jung, Y.K.; Lee, B.: Design of adaptive optimal load circuit for maximum wireless power transfer efficiency, in *Asia-Pacific Microwave Conf. Proc. (APMC)*, (2013), 1221–1223.
- [17] Lee, J.; Lim, Y.-S.; Yang, W.-J.; Lim, S.-O.: Wireless power transfer system adaptive to change in coil separation. *IEEE Trans. Antennas Propag.*, **62** (2014), 889–897.
- [18] Heebl, J.D.; Thomas, E.M.; Penno, R.P.; Grbic, A.: Comprehensive analysis and measurement of frequency-tuned and impedance-tuned wireless non-radiative power-transfer systems. *IEEE Antennas Propag. Mag.*, (2014), **56**, 44–60.
- [19] Lee, H.-M.; Kwon, K.-Y.; Li, W.; Ghovanloo, M.: A power-efficient switched-capacitor stimulating system for electrical/optical deep brain stimulation. *IEEE J. Solid-State Circuits*, (2015), **50**, 360–374.
- [20] Buisman, K. et al.: Varactor topologies for RF adaptivity with improved power handling and linearity, in *Proc. IEEE/MTT-S Int. Microwave Symp.*, (2007), 319–322.
- [21] Buisman, K.; Cong, Huang ; Zampardi, P.J.; de Vreede, L.C.N.: RF power insensitive varactors. *IEEE Microw. Wireless Compon. Lett.*, (2012), **22**, 418–420.
- [22] Ogawa, K.; Oodachi, N.; Obayashi, S.; Shoki, H.: a study of efficiency improvement of wireless power transfer by impedance matching, in *IEEE MTT-S Int. Microwave Workshop Series on Innovative Wireless Power Transmission: Technologies, Systems, Applications (IMWS-IWPT)*, May (2012), 155–157.
- [23] Sample, A.P.; Waters, B.H.; Wisdom, S.T.; Smith, J.R.: Enabling seamless wireless power delivery in dynamic environments. *Proc. IEEE*, **101** (6) (2013), 1343–1358.
- [24] Lai, X.; Yuan, F.: Remote calibration of wireless power harvest, in *MWSCAS*, (2013), 501–504.
- [25] Saltanovs, R.: Multi-capacitor circuit application for the wireless energy transmission system coils resonant frequency adjustment, in *IEEE Wireless Power Transfer Conf. (WPTC)*, (2015), 1–3.